

## Nanopore Formation and Phosphatidylserine Externalization in a Phospholipid Bilayer at High Transmembrane Potential

P. Thomas Vernier,<sup>\*,†</sup> Matthew J. Ziegler,<sup>‡</sup> Yinghua Sun,<sup>‡</sup> Wenji V. Chang,<sup>‡</sup> Martin A. Gunderson,<sup>#</sup> and D. Peter Tieleman<sup>§</sup>

*Departments of Electrical Engineering and Chemical Engineering and Materials Science, Viterbi School of Engineering, University of Southern California, Los Angeles, California 90089-0271, MOSIS, Information Sciences Institute, Viterbi School of Engineering, University of Southern California, Marina del Rey, California 90292, and Department of Biological Sciences, University of Calgary, Calgary, Alberta, Canada T2N 1N4*

Received December 30, 2005; E-mail: vernier@mosis.org

Externalization of phosphatidylserine (PS), a phospholipid normally confined to the inner leaflet of the plasma membrane, follows exposure of biological cells to high-field electric pulses of <100 ns duration.<sup>1</sup> Nanosecond, megavolt-per-meter pulses cause intracellular calcium release<sup>2,3</sup> and induce apoptosis,<sup>4</sup> but membrane permeability to propidium iodide, a standard electroporation indicator, is not observed. Nanoelectropulse-driven PS translocation is immediate and distinct from the PS externalization that is symptomatic of apoptosis.<sup>5</sup> Although nanosecond pulses do not cause conventional electroporation, we have recently observed YO-PRO-1 influx, a sensitive fluorescent reporter of membrane integrity, after exposure of cells to multiple 4 ns, 8 MV/m pulses, indicating a perturbative but not disruptive breaching of the membrane hydrophobic barrier.<sup>6</sup>

We present here observations of localized PS externalization in response to nanosecond electric pulses (imaged for the first time with annexin V binding), and we correlate these experimental data with molecular dynamics (MD) simulations of dioleoylphosphatidylcholine–dioleoylphosphatidylserine (DOPC–DOPS) asymmetric membranes in high electric fields. We demonstrate the association between field-driven poration and PS translocation, and we draw a line of continuity from experiments on living cells to mathematical models of pore formation in lipid bilayers, leading to the conclusion that nanoelectropulse-driven PS externalization (1) occurs on a nanosecond time scale, (2) is restricted to the anode-facing pole of the cell, and (3) is intimately connected with and dependent on nanopore formation.

Fluorescence microscopy with the fluorescent-tagged PS-binding protein annexin V and FM1-43, a cationic fluorochrome that partitions between the aqueous medium and the outer leaflet of the cytoplasmic membrane, where its fluorescence greatly increases,<sup>7</sup> reveals nanoelectropulse-induced perturbations associated with PS externalization localized exclusively at the anode-facing pole of the cell immediately after pulse exposure (Figure 1). Because the kinetics and sensitivity of these imaging methods permit only micrometer- and millisecond-scale resolution of post-pulse membrane restructuring<sup>8</sup> and cannot be used to visualize molecular events with nanosecond resolution, we turned to MD to provide insight into the mechanisms of nanosecond pulse-driven poration and PS translocation.

Previous MD electroporation studies show that, with electric fields of 400 mV/nm, water intrusions into the bilayer extend across the membrane within nanoseconds, with phospholipid headgroups following the initial water chain to line the resulting hydrophilic

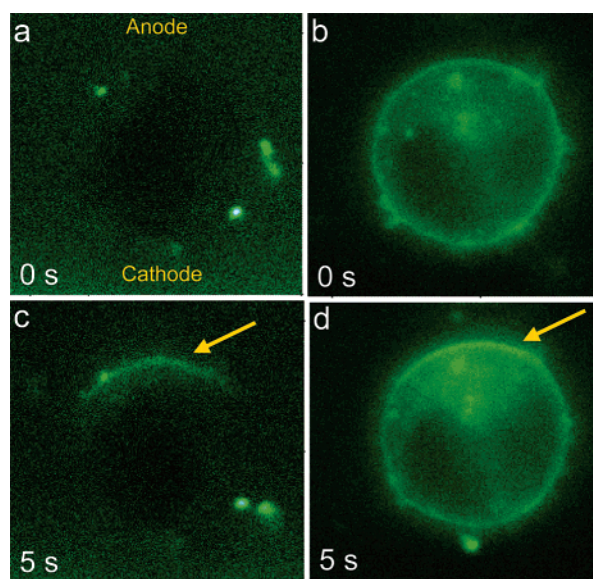


**Figure 1.** PS externalization in RPMI 8226 human multiple myeloma cells after exposure to 4 ns, 8 MV/m pulses. Separate cells stained with annexin V-FITC (a) and FM1-43 (b) are shown before and 5 s after pulse delivery (c,d). The anode (positive terminal) is at the top of each image; the cathode is at the bottom. Fluorescence indicating PS translocation appears at the anode-facing pole of the cell. Note correspondence of the regions of pulse-induced annexin V binding and FM1-43 fluorescence intensification.

pore.<sup>9,10</sup> In coarse-grained simulations, poration and PS externalization occur during a single 10 ns pulse.<sup>11</sup>

Using Gromacs-generated atomic resolution representations of a DOPC–DOPS bilayer in water at 300 K, 1 bar, we ran simulations with varying field strengths and polarities. One bilayer face contains 64 DOPC molecules; the other, representing a cell membrane internal leaflet, contains 4 DOPS and 60 DOPC molecules, with 4 Na<sup>+</sup> ions to balance the DOPS charge. Parameters and simulation methods are as previously described for homogeneous bilayers<sup>9,12</sup> (see Supporting Information). Snapshots from a typical simulation are shown in Figure 2.

With an electric field of 450 mV/nm, water intrusion occurs in ~5 ns (Figure 2a), from the cathode side of the membrane. Within 0.5 ns, a column of dipole-aligned water molecules (Figure S1) spans the membrane interior, and phospholipid headgroups begin to realign along the new aqueous surface (Figure 2b). By 6 ns, PS headgroups are migrating along the walls of the incipient pore (Figure 2c) toward the anode (Figure 2d). In <7 ns, the first PS molecule crosses the 5 nm span of the lipid membrane interior. In 30 simulations with fields from 200 to 800 mV/nm, water defects appear predominantly at the cathode-facing leaflet of the bilayer,

<sup>†</sup> MOSIS, USC-ISI.

<sup>‡</sup> Department of Chemical Engineering and Materials Science, USC.

<sup>#</sup> Department of Electrical Engineering, USC.

<sup>§</sup> University of Calgary.

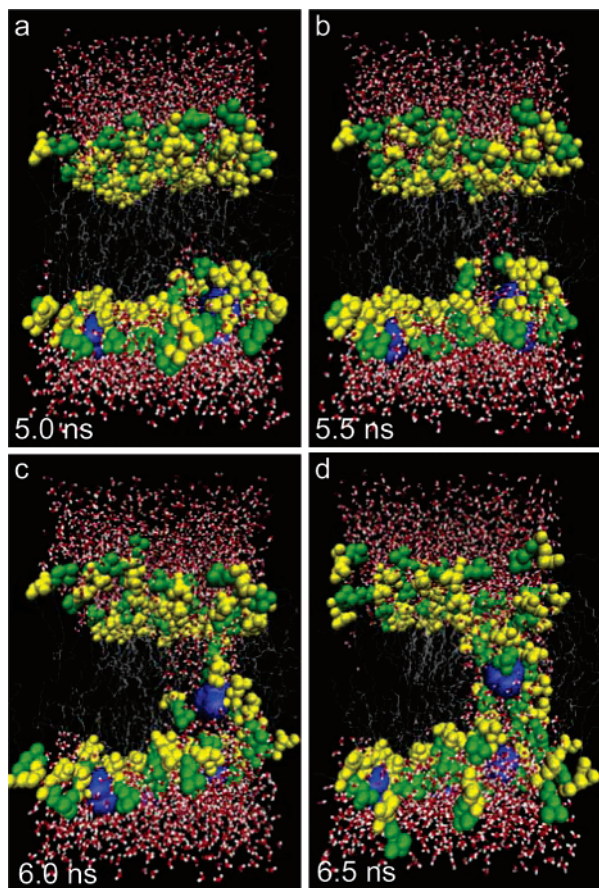


**Figure 2.** Nanoporation and PS translocation in a DOPC–DOPS bilayer in a 450 mV/nm electric field, directed from top to bottom, with the positive electrode at the top. Water atoms are red (O) and white (H); phospholipid tails are gray; glycerophosphate atoms are yellow, choline atoms green, serine atoms blue. Serine atoms are enlarged to enhance visibility.

regardless of the location of PS, and PS translocates only after pore formation and always to the side of the membrane facing the positive electrode, as in live cell observations<sup>8</sup> (Figure 1). Pore formation occurs more rapidly as the field increases, and in some higher field cases water intrusion occurs also at the anode side of the membrane. Poration is observed in <5 ns in 21 out of 24 simulations when the field is 450 mV/nm or greater. PS translocation occurs only along pore walls and only when the field direction is as indicated in Figure 2. PS does not facilitate water pore formation, consistent with the suggestion that interactions in the hydrophobic interior of the membrane dominate the relative ease of propagation of a water column into the bilayer.<sup>9</sup>

Pulse-driven PS externalization appears to be an electrophoretic transport of PS headgroups through hydrophilic pores. Switching the field polarity during a simulation reverses the direction of this interleaflet electrophoresis.

Why such a large electric field? At a porating potential of 1 V, the area occupied by pores is <1% of the cell surface area.<sup>13</sup> To ensure that we observe pore formation during a simulation, we must increase either the simulated area (22 nm<sup>2</sup>) or the simulation time — both computationally expensive — or, since pore density in the stochastic model<sup>14</sup> is dependent on transmembrane voltage ( $\Delta\psi_m$ ),<sup>15</sup> increase  $\Delta\psi_m$ .

On a microsecond scale, the conductive pores produced by suprphysiological transmembrane potentials clamp the voltage at  $\sim 1$  V,<sup>16</sup> but current models allow higher potentials for at least a few nanoseconds.<sup>17,18</sup> A simulated  $\psi_m$  of 3.4 V (450 mV/nm)<sup>8</sup> produces poration and PS translocation in <10 ns. Simulations that represent the poration-driven drop in  $\psi_m$  will be required to establish how well this reflects the experimental situation. At 1.5 V (200 mV/nm), we see transitory water defects but no pores, even in multiple repetitions, consistent with the exponential dependence on  $\Delta\psi_m$  in the stochastic pore model.

These simulations of phospholipid bilayers, combined with evidence from fluorescence microscopic imaging observations of living cells, demonstrate that a transmembrane electric field can produce nanometer-diameter hydrophilic pores within nanoseconds and that the anionic phospholipid PS is driven electrophoretically through the pores. Further explication of the energetic and kinetic details of these processes, with systems that more closely represent the complexity of a living cell membrane, will lead to improved methods for electroporation in research and clinical applications, and to a better understanding of PS translocation mechanisms in apoptosis and signal transduction.

**Acknowledgment.** This work was supported by the Air Force Office of Scientific Research. Computing resources were provided by the USC Center for High Performance Computing and Communications (<http://www.usc.edu/hpcc/>). P.T.V. and M.J.Z. are supported by MOSIS, Information Sciences Institute, USC. Work in D.P.T.'s group is supported by NSERC. D.P.T. is an AHFMR Senior Scholar, CIHR New Investigator, and Sloan Foundation Fellow.

**Supporting Information Available:** Simulation details and methods. This material is available free of charge via the Internet at <http://pubs.acs.org>.

## References

- (1) Vernier, P. T.; Sun, Y.; Marcu, L.; Craft, C. M.; Gundersen, M. A. *Biophys. J.* **2004**, *86*, 4040–4048.
- (2) Vernier, P. T.; Sun, Y.; Marcu, L.; Salemi, S.; Craft, C. M.; Gundersen, M. A. *Biochem. Biophys. Res. Commun.* **2003**, *310*, 286–295.
- (3) White, J. A.; Blackmore, P. F.; Schoenbach, K. H.; Beebe, S. J. *J. Biol. Chem.* **2004**, *279*, 22964–22972.
- (4) Beebe, S. J.; Fox, P. M.; Rec, L. J.; Willis, E. L.; Schoenbach, K. H. *FASEB J.* **2003**, *17*, 1493–1495.
- (5) Vernier, P. T.; Li, A. M.; Marcu, L.; Craft, C. M.; Gundersen, M. A. *IEEE Trans. Dielectr. Electr. Insul.* **2003**, *10*, 795–809.
- (6) Vernier, P. T.; Sun, Y.; Wang, J.; Thu, M. M.; Garon, E.; Valderrabano, M.; Marcu, L.; Koefler, H. P.; Gundersen, M. A. *Proc. IEEE Eng. Med. Biol. Soc. 27th Int. Conf.*, Shanghai, 2005.
- (7) Zweifach, A. *J. Cell Biol.* **2000**, *148*, 603–614.
- (8) Vernier, P. T.; Sun, Y.; Marcu, L.; Craft, C. M.; Gundersen, M. A. *FEBS Lett.* **2004**, *572*, 103–108.
- (9) Tieleman, D. P. *BMC Biochem.* **2004**, *5*, 10.
- (10) Tarek, M. *Biophys. J.* **2005**, *88*, 4045–4053.
- (11) Hu, Q.; Joshi, R. P.; Schoenbach, K. H. *Phys. Rev. E* **2005**, *72*, 031902.
- (12) Tieleman, D. P.; Leontiadou, H.; Mark, A. E.; Marrink, S. J. *J. Am. Chem. Soc.* **2003**, *125*, 6382–6383.
- (13) Chernomordik, L. V.; Sukharev, S. I.; Abidor, I. G.; Chizmadzhev, Y. A. *Biochim. Biophys. Acta* **1983**, *736*, 203–213.
- (14) Sugar, I. P.; Neumann, E. *Biophys. Chem.* **1984**, *19*, 211–25.
- (15) DeBruin, K. A.; Krassowska, W. *Ann. Biomed. Eng.* **1998**, *26*, 584–596.
- (16) Teissie, J.; Tsong, T. Y. *Biochemistry* **1981**, *20*, 1548–1554.
- (17) DeBruin, K. A.; Krassowska, W. *Biophys. J.* **1999**, *77*, 1213–1224.
- (18) Stewart, D. A.; Gowrishankar, I. R.; Weaver, J. C. *IEEE Trans. Plasma Sci.* **2004**, *32*, 1696–1708.

JA0588306